Distribution of nutrients and dissolved organic matter in a eutrophic equatorial estuary, the Johor River and East Johor Strait

Amanda Y. L. Cheong[1,*], Kogila Vani Annammala[2], Ee Ling Yong[2], Yongli Zhou[1,¶], Robert S. Nichols[1,†], Patrick Martin[1]

[1]Asian School of the Environment, Nanyang Technological University, 639798, Singapore
[2]Department of Water and Environmental Engineering, Faculty of Civil Engineering, Universiti Teknologi Malaysia, 81310 Johor, Malaysia
[*]Present address: AON Singapore, 068804 Singapore
[¶]Present address: Department of Geography, University of Hong Kong, Hong Kong SAR, China
[†]Present address: DHI Water & Environment (S) Pte Ltd, 608526 Singapore

Correspondence to: Patrick Martin (pmartin@ntu.edu.sg)

Abstract. Estuaries have strong physicochemical gradients that lead to complex variability and often high rates of biogeochemical processes, and are also often impacted by humans. Yet our understanding of estuarine biogeochemistry remains skewed towards temperate latitudes. We examined seasonal and spatial variability in dissolved organic matter (DOM) and nutrients along a partly eutrophic, mixed agricultural/urban estuary system in Southeast Asia, the Johor River and the East Johor Strait. Dissolved organic carbon (DOC) and coloured DOM (CDOM) showed non-conservative mixing, indicating significant DOM inputs along the estuary. The CDOM spectral slopes and CDOM:DOC ratios suggest that terrigenous, soil-derived DOM dominates along the Johor River, while phytoplankton production and microbial recycling are important DOM sources in the Johor Strait. The CDOM properties were not unambiguous source indicators in the eutrophic Johor Strait, likely due to heterotrophic CDOM production. Nitrate concentrations showed conservative mixing, while nitrite concentrations peaked at intermediate salinities of 10–25. Ammonium concentrations decreased with salinity in the Johor River, but increased up to 50 µmol l^{-1} in the Johor Strait, often dominating the dissolved inorganic nitrogen (DIN) pool. Phosphate concentrations were low (<0.5 µmol l^{-1}) throughout the Johor River, but increased in the Johor Strait, where DIN:phosphate ratios were typically ≥16:1. The Johor River and Johor Strait are clearly not simply part of the same estuarine mixing continuum. Our data also suggest that the Johor Strait may experience phosphorus limitation, and that internal recycling is likely important for maintaining high nutrient concentrations in the Johor Strait.

1 Introduction

The biogeochemical functioning of estuaries and coastal waters is greatly influenced by terrestrial inputs as well as by biogeochemical transformations taking place along the land–ocean aquatic continuum (Bianchi and Morrison, 2023; Martin and Bianchi, 2023; Voss et al. 2011). These fluxes and biogeochemical processes can be greatly affected by increasing coastal development, changing land-use practices, and climatic changes. Because of the ecological and economic value of estuaries and coastal waters, it is important to better understand these fluxes and processes and how they are changing. Southeast Asia is experiencing amongst the highest rates of coastal urbanisation (Neumann et al., 2015), land-use change (Hansen et al., 2013; Stibig et al., 2014), and increased nutrient pollution (Sinha et al., 2019). However, our understanding of estuarine and coastal biogeochemistry remains skewed towards temperate latitudes (Lønborg et al., 2021b; Vieillard et al., 2020). Thus, although

tropical estuaries receive a large fraction of the global land–ocean fluxes of carbon, nutrients, and sediments (Jennerjahn, 2012),
many tropical estuaries are comparatively poorly studied.

Eutrophication of estuaries and coastal waters due to anthropogenic nutrient input is a world-wide problem, resulting in phytoplankton blooms, oxygen depletion and dead zones (Altieri et al., 2017; Le Moal et al., 2019). Globally, agriculture is the main source of anthropogenic N and P input, but many other point and non-point sources may be important in a given location (Beusen et al., 2016; Le Moal et al., 2019). Anoxic conditions in eutrophic systems can promote nutrient recycling, especially the release of phosphorus from sediments (Sulu-Gambari et al., 2018; Ballagh et al., 2020). Although nitrogen is usually lost by denitrification and anaerobic ammonia oxidation (anammox) under anoxic conditions (Voss et al., 2011; Zhu et al., 2013; Teixeira et al., 2016), dissimilatory nitrate reduction to ammonia (DNRA) can also take place and recycle nitrogen (Dong et al., 2011; Bernard et al., 2015). Importantly, the relative rates of these biogeochemical processes may differ between tropical and temperate systems (Dong et al., 2011; Li et al., 2019).

Estuaries also receive large fluxes of terrestrial organic carbon, partly as a result of human activities (Regnier et al., 2022; Martin and Bianchi, 2023). Tropical rivers are particularly significant sources of dissolved organic carbon (DOC) to the ocean (Dai et al., 2012), with mangroves thought to be a disproportionally large source of terrigenous DOC (Dittmar et al., 2006). Terrigenous DOC is typically rich in coloured dissolved organic matter, CDOM (Coble, 2007; Massicotte et al., 2017), and terrigenous CDOM typically has distinct optical properties compared to CDOM in the open ocean and coastal seas (Stedmon and Nelson, 2015). Specifically, CDOM spectral slopes at ultraviolet wavelengths (Helms et al., 2008) and specific UV absorbance at 254 nm, $SUVA_{254}$ (Traina et al., 1990; Weishaar et al., 2003) have become widely used metrics to distinguish terrigenous dissolved organic matter (DOM) from autochthonous DOM produced in aquatic environments (Asmala et al., 2016; Fichot and Benner, 2011; Lønborg et al., 2021a; Zhou et al., 2021).

Tropical peatlands are the largest source of terrigenous DOC to the coastal ocean in Southeast Asia. Most research on land–ocean DOC fluxes in this region has therefore focused on peatland-draining rivers (Baum et al., 2007; Wit et al., 2015; Martin et al., 2018; Rixen et al., 2022; Sanwlani et al., 2022), leaving us with a more limited understanding of the concentrations and optical properties of DOM in non-peat-draining estuaries. Moreover, there have been few studies of the distributions of DOM and nutrients across more urbanised and eutrophic estuaries in Southeast Asia.

Here, we examined the seasonal dynamics and mixing behaviours of DOC, CDOM, and dissolved inorganic nutrients across salinity gradients in the Johor River estuary and the eutrophic East Johor Strait, at the southern tip of the Malay Peninsula. The objectives of our study were to identify the sources (terrigenous versus marine) and cycling behaviour of these substances, determine whether there is seasonal variation, and examine how the optical properties of CDOM delivered by the Johor River compare to those in the eutrophic Johor Strait.

2 Methods

2.1 Study Area

The Johor River (Fig. 1) is around 123 km long and provides a crucial freshwater source for Johor State and for Singapore (Kang and Kanniah, 2022). The Johor River drains into a large estuary to which several other rivers also contribute, with a

total drainage basin area of around 2640 km^2, before flowing southwards past the East Johor Strait into the Singapore Strait (Fig. 1). The main land cover in the catchment is agricultural, especially rubber and oil palm plantation, with some urban and industrial land use (Kang and Kanniah, 2022; Fig. 1a). The Johor River estuary has fringing mangroves along most of its length, providing a narrow buffer zone to the mostly agricultural areas. Sand extraction takes place in the river, and in the lower parts of the estuary, small-scale aquaculture is practiced. Along the Johor River and its estuary, wastewater treatment plants and fertiliser run-off are sources of ammonia, with point-source inputs via wastewater being more important during drier periods and non-point-source inputs from fertiliser use more important during wetter periods (Samsudin et al., 2017; Pak et al., 2021).
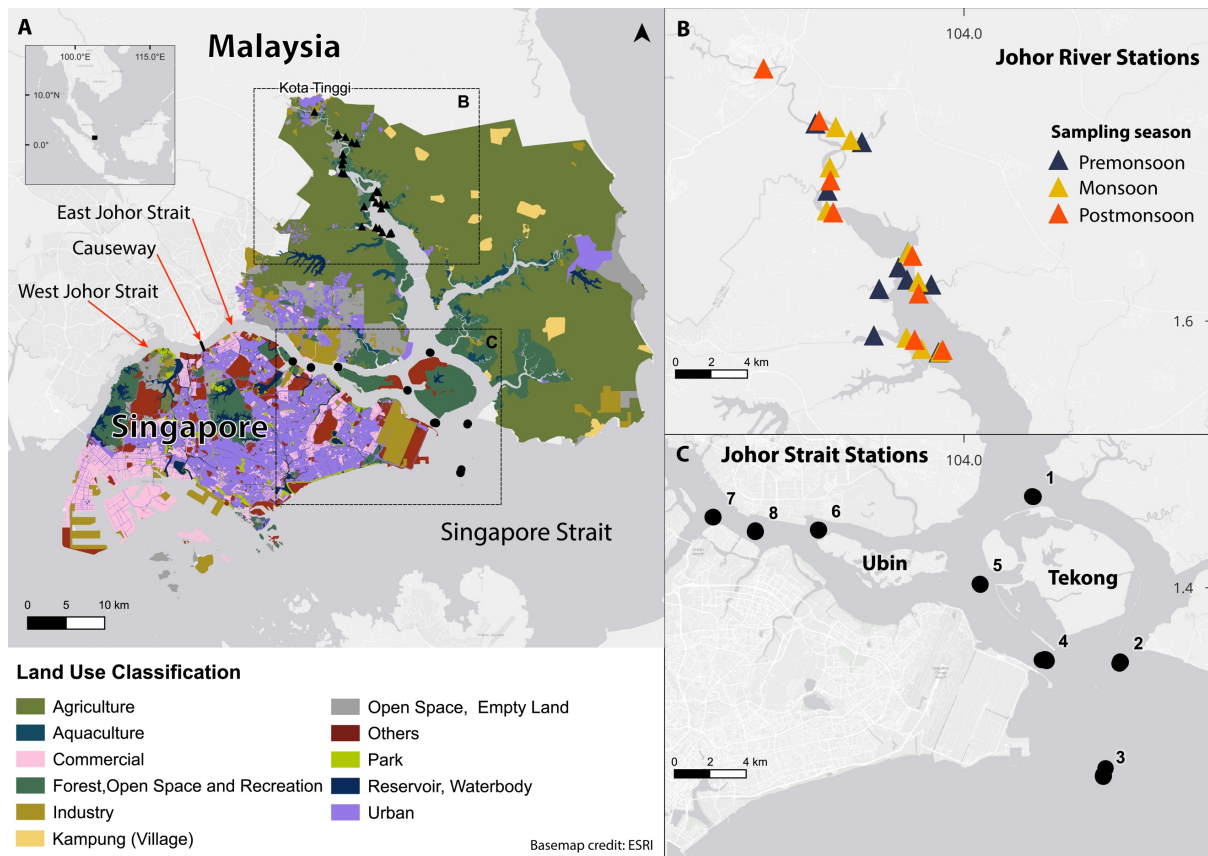
Figure 1. Map of the study region. Triangles show stations in the Johor River estuary, points show stations in the East Johor Strait. (A) Land use in the area around the Johor River estuary and East Johor Strait. Land use for Malaysia was taken from GeoJohor Johor land-use portal (http://geoportal.johor.gov.my/en/, accessed 11 December 2022), land use for Singapore was taken from the Singapore Urban Redevelopment Authority master plan (https://www.ura.gov.sg/maps/?service=mp, accessed 10 January 2024). Dashed boxes show locations for panels (B,C). (B) Station locations sampled in the Johor River estuary. (C) Station locations sampled in the East Johor Strait.

The Johor Strait is the narrow (1–2 km wide) channel that separates Singapore from Malaysia (Figs. 1a,b). It is divided by a causeway into the East and West Johor Strait, with limited water exchange between the two. The East Johor Strait receives run-off from both Malaysia and Singapore, with both sides of the Strait dominated by urban and industrial land use. Fringing mangroves are also found especially in the eastern part of the Strait (Fig. 1a). Aquaculture is practiced especially around the island of Pulau Ubin, which is mostly a forested nature reserve. Both the East and West Johor Strait are eutrophic water bodies, and occasional harmful algal blooms by diatoms and dinoflagellates have been reported (Gin et al., 2000; Chénard et al., 2019; Kok and Leong, 2019; Wijaya et al., 2023).

Singapore and Malaysia experience two monsoon seasons: the northeast monsoon from November to March and the southwest monsoon from mid-May to mid-September. Rain falls year-round, but there is a distinct increase in precipitation during the early northeast monsoon (mid-November to early January), followed immediately by the driest time of year in the late northeast and intermonsoon period (February to March/April). Average monthly rainfall for 2000–2020 and monthly rainfall during our study period was calculated over the area 1.2°N 103.6°E to 1.8°N 104.4°E, using data from the Integrated Multi-Satellite Retrievals for Global Precipitation Measurement (IMERG) Final Precipitation L3 0.1°-resolution product processed by the Royal Netherlands Meteorological Institute (Huffman et al., 2014). Discharge from the Johor River at the gauging station in Rantau Panjang (1.781°N 103.746°E) was obtained from the Department of Irrigation and Drainage, Malaysia. We designated data collected prior to December 2017 as pre-monsoon, data collected during December and January as monsoon, and data collected after January 2018 as post-monsoon, and distinguish between these three periods in our plotting and analysis.

2.2 Sampling

We collected surface water samples in the East Johor Strait at eight stations approximately monthly from August 2017 to June 2018 (Fig. 1c). Samples were collected in the Johor River on 03–04 November 2017 (pre-monsoon, sampled before the monsoon peak in river discharge; see Figure 2), 10 January 2018 (monsoon) and 06 March 2018 (post-monsoon) at 8–10 stations (Fig. 1b). Water samples were collected either using a hand-held polyethylene jug (Johor River) or a Niskin bottle (Johor Strait, at 1 m depth). At each station, a conductivity-temperature-depth (CTD) and chlorophyll-a (chl-a) fluorescence profile was taken using a Valeport FastCTD, and we use the average values over the upper 1 m in our analysis. Salinity is reported on the practical salinity scale and is therefore unitless. Due to a CTD malfunction on 09 March 2018, CTD profiles could not be taken in the Johor Strait on this date, and salinity was instead measured using an optical refractometer.

Samples for dissolved inorganic nutrients were syringe-filtered (0.22 µm, Pall Acrodisc) in the field into acid-rinsed 15-mL polypropylene centrifuge tubes, immediately frozen in a dry shipper, then stored at -20°C until analysis. For DOC and CDOM, unfiltered water was stored in pre-combusted (450°C, 4 h) amber borosilicate bottles at ambient temperature in the dark and then filtered back on land on the same day through Whatman Anodiscs (0.2 µm, 45 mm diameter) in an all-glass filtration system. The filtration system was rinsed with 1 M HCl and ultrapure deionised water (Elga 18.2 MΩ cm^{-1}; referred to as DI water below) prior to every sample. DOC and CDOM samples were then stored in amber borosilicate vials at +4°C until analysis; DOC samples were acidified with 50% H_2SO_4 immediately after filtration.

2.3 Sample analyses

2.3.1 Dissolved organic carbon (DOC) analysis

Samples were analysed within three months of collection as non-purgeable organic carbon on a Shimadzu TOC-L system with the Shimadzu high-salt kit, using potassium hydrogen phthalate for calibration. Instrumental detection limits were below the lowest standard concentration of ~20 µmol l^{-1}, and thus much lower than the lowest measured sample of 71 µmol l^{-1}. Deep-sea water certified reference material from the University of Miami (42–45 µmol l^{-1}) was analysed with every run, and returned a long-term mean and standard deviation of 48 ± 3.5 µmol l^{-1}.

2.3.2 Coloured dissolved organic matter (CDOM) analysis

CDOM absorption spectra (230-900 nm) were measured with a Thermo Evolution300 dual-beam spectrophotometer against a DI water reference using 10-cm quartz cuvettes. The absorbance spectra were corrected for instrument baseline drift following Green and Blough (1994), smoothed using a loess function, and converted to Napierian absorption coefficients using Equation (1):

$$a_\lambda = 2.303 \times \frac{A_\lambda}{l} \tag{1}$$

where a_λ is the absorption coefficient (m^{-1}), A_λ is the absorbance, l is the cuvette path length (in m), and subscript λ indicates wavelength. We then calculated the spectral slopes between 275–295 nm ($S_{275-295}$), between 350–400 nm ($S_{350-400}$), and the slope ratio S_R (ratio of $S_{275-295}$ to $S_{350-400}$) using linear regressions of the natural log-transformed absorption against wavelength following Helms et al. (2008). The specific UV absorbance at 254 nm (SUVA$_{254}$) was determined by dividing the decadic absorption at 254 nm (i.e., the absorbance per metre) by the DOC concentration (in mg l^{-1}). CDOM data processing was carried out in MATLAB. We report CDOM absorption at 350 nm (a_{350}) as a measure of CDOM concentration.

2.3.3 Nutrient analysis

Samples for NO$_x$ (i.e., NO$_3^-$ + NO$_2^-$), NO$_2^-$, PO$_4^{3-}$, Si(OH)$_4$, and NH$_4^+$ were thawed and analysed on a SEAL AA3 segmented-flow autoanalyzer following SEAL methods G172, G173, G297, and G177. NH$_4^+$ was measured fluorometrically (Kérouel and Aminot, 1997). Detection limits were 0.05 µmol l^{-1} (NO$_x$), 0.01 µmol l^{-1} (NO$_2^-$), 0.03 µmol l^{-1} (PO$_4^{3-}$), 0.10 µmol l^{-1} (Si(OH)$_4$), and 0.25 µmol l^{-1} (NH$_4^+$). Dissolved inorganic nitrogen (DIN) was calculated as NO$_x$ + NH$_4^+$. Where measurements were below the detection limit (1 sample for PO$_4^{3-}$, and 25 samples for NH$_4^+$), the concentration was assumed to be 0.5 x the detection limit. The nutrient data for the Johor River samples were previously published by Liang et al. (2020).

2.4 Conservative mixing models and statistical analysis

For DOC and CDOM, we used a two-endmember mixing model to calculate concentrations expected under conservative mixing across the salinity gradient. The freshwater endmember values were taken from the station furthest upriver (Kota Tinggi, 1.6973°N 103.9358°E), while the marine endmember values were taken from the southernmost station (Station 3 in Fig. 1c, where the Johor Strait opens into the Singapore Strait). The mixing models were calculated for DOC and for CDOM absorption spectra using Equation 2:

$$X_{mix} = f_{riv}X_{riv} + (1 - f_{riv})X_{mar} \tag{2}$$

Where X_{mix} is the predicted DOC concentration or CDOM absorption at each intermediate salinity, f_{riv} is the fraction of freshwater at that salinity, and X_{riv} and X_{mar} are the riverine and marine endmember values for DOC or CDOM absorption. The mixing models were calculated at salinity increments of 1. Because CDOM spectral slopes change non-linearly during conservative mixing, we calculated the predicted absorption spectrum at every wavelength using Eq. 2 and then calculated the predicted spectral slope parameters from the predicted spectra, following Stedmon and Markager (2003).

Where two variables clearly showed a coherent and linear relationship to each other, we used linear regression analysis to test for a significant relationship, and report the regression equation together with r^2 and p-values. In cases where there was greater scatter or visible non-linearity, we used Spearman's rank correlation analysis instead, and report the rho- and p-values.

3 Results

3.1 Rainfall pattern and river discharge at Kota Tinggi, Johor

Rainfall across the study region (Fig. 2a) is relatively high year-round, but with a distinctly wetter period during the early part
of the northeast monsoon (Nov–Jan) and a drier period during the late northeast monsoon (Feb–Mar). During our study period,
175   November 2017 was the wettest month with 407 mm of rain, while February 2018 was the driest month with 106 mm of
rainfall. The overall monthly rainfall distribution during our study period was similar to the long-term average from 2001 to
2020.
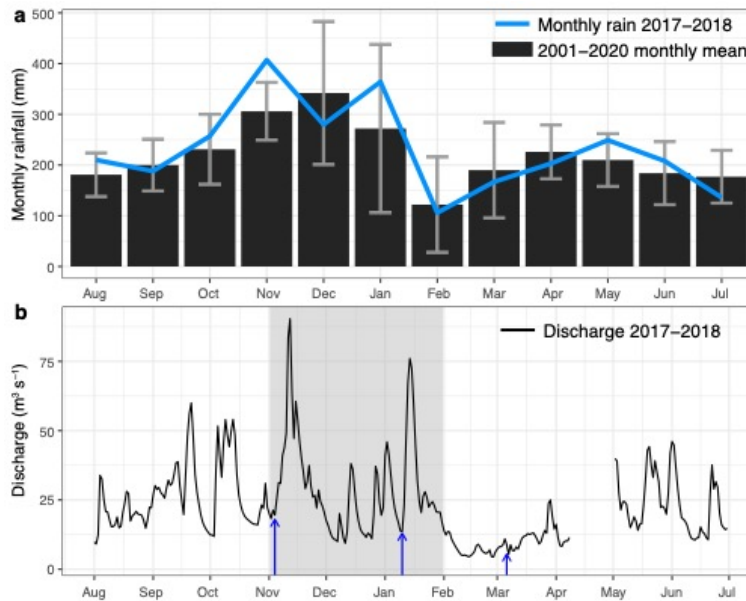
180   **Figure 2. (a) Monthly rainfall across the study region during the period August 2017 to July 2018 (blue line), and long-term mean
monthly rainfall from 2001–2020 (black bars). Grey error bars indicate 1 standard deviation of the long-term mean. (b) Daily river
discharge for the Johor River measured at Rantau Panjang hydrological station (1.781°N, 103.746°E). Blue arrows indicate the
Johor River sampling dates (for pre-monsoon sampling, arrow indicates 04 Nov).**

185   Discharge of the Johor River measured at Rantau Panjang showed a distinct minimum during the dry period in the late northeast
monsoon (February–March 2018; Fig. 2b). Discharge during the early northeast monsoon showed two distinct peaks, on 12
November 2017 (90.4 m³ s⁻¹) and 14 January 2018 (76.0 m³ s⁻¹), but discharge was otherwise not notably elevated during
November–January relative to other periods, except compared to the late northeast monsoon (February–March; Fig. 2b). Note
that the pre-monsoon sampling in the Johor River was conducted on 03–04 November 2017, just before the river discharge
190   began to increase (Figure 2b).

3.2 Temperature and Salinity

In the Johor River, surface salinity ranged from 0.5–26.8 (November, pre-monsoon), 0–16.1 (January, monsoon), and 4–28.3
(March, post-monsoon), with lowest salinity always furthest upstream at Kota Tinggi town (Supplementary Figures 1–3).
Salinity ranged from 21.6–32.4 for all stations in the Johor Strait, with lowest salinity (mean 25.9, range 21.6–29.0) typically
195   found at Station 1, where the Johor River estuary meets the Johor Strait, while Station 3, located at the entrance to the Singapore
Strait, had the highest salinity (mean 30.9, range 30.0–32.4).

Surface temperature varied little and spanned nearly identical ranges in the Johor River (26.7–30.2°C) and the Johor Strait (26.5–31.6°C), with the lower values found during the northeast monsoon, but otherwise no distinct seasonal variation.

3.2 Dissolved organic matter distribution

DOC concentrations ranged from 101 µmol l^{-1} to 186 µmol l^{-1} in the Johor River (average 136 µmol l^{-1}) and between 71 µmol l^{-1} to 208 µmol l^{-1} in the Johor Strait (average 113 µmol l^{-1}; Fig. 3a). DOC concentrations in the Johor River estuary showed a clear non-conservative mixing pattern, indicative of additional DOC sources to the estuary, and only showed a decrease after salinity exceeded about 22. In the Johor Strait, DOC concentrations showed a relatively linear decrease with salinity, with lowest values consistently found at Johor Strait Station 3 (average of 79 µmol l^{-1}), closest to the open sea in the Singapore Strait (c.f. Fig. 1). Seasonal variability was not pronounced, although at salinities between 5 and 25, DOC concentrations were lower during the northeast monsoon. Moreover, five stations in the Johor Strait showed elevated DOC concentrations relative to their salinity (four stations in February 2018, one station in June 2018), which were associated with phytoplankton blooms (see Section 3.3). Overall, the distribution of DOC did not follow simple 2-endmember conservative mixing between the Johor River and the Singapore Strait: essentially all stations along the salinity gradient had higher than predicted DOC concentrations (Fig. 3a).
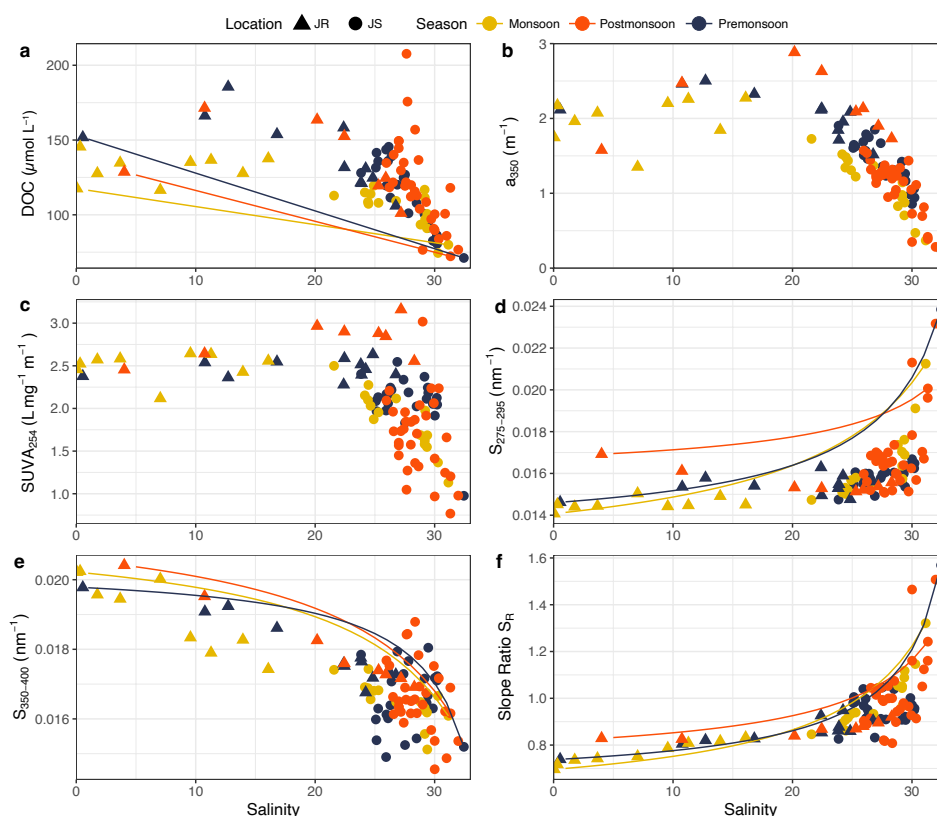
Figure 3. Distribution against salinity of (a) DOC concentration, (b) CDOM a$_{350}$, (c) SUVA$_{254}$, (d) CDOM spectral slope S$_{275-295}$, (e) CDOM spectral slope S$_{350-400}$, (f) CDOM spectral slope ratio S$_R$. The solid triangles represent data from the Johor River, circles represent data from the Johor Strait, and symbol colours indicate sampling season. Solid lines indicate theoretical conservative mixing lines calculated for each sampling season.

CDOM a$_{350}$ and SUVA$_{254}$ showed a very similar distribution to DOC, with relatively stable values up to salinity 25 in the Johor River and then a linear decrease with salinity above 25. CDOM a$_{350}$ ranged from 1.35–2.88 m^{-1} in the Johor River, and from

0.25 – 1.90 m^{-1} in the Johor Strait (Fig. 3b), while SUVA$_{254}$ ranged from 2.1–3.2 l mg^{-1} m^{-1} throughout the Johor River and from 0.8–3.0 l mg^{-1} m^{-1} in the Johor Strait (Fig. 3c). The CDOM spectral slope S$_{275-295}$ showed low values (0.0141 – 0.0176 nm^{-1}) up to salinity of 30 but increased to 0.0196–0.0239 nm^{-1} at the highest salinities (Fig. 3d). The spectral slope S$_{350-400}$ showed a steadily decreasing trend over the salinity gradient, from ≥0.0194 nm^{-1} at salinities below 7 to values ranging between
225   0.0146–0.0188 nm^{-1} in the Johor Strait (Fig. 3e). The slope ratio, S$_R$, consequently mirrored the pattern in S$_{275-295}$, with values consistently below 1.0 up to salinity of 25, and then increasing to between 1.0 – 1.6 at the higher salinities (Fig. 3f). There was only limited seasonal variability in the CDOM parameters: values of a_{350}, S$_{275-295}$, and S$_{350-400}$ were slightly lower during the northeast monsoon at salinities between 5–25 than in the other seasons, but this was not seen in S$_R$ or in SUVA$_{254}$. S$_{275-295}$ clearly departed from the conservative mixing models, while S$_{350-400}$ and S$_R$ showed somewhat closer agreement (Fig. 3). The
230   five stations with high DOC concentrations due to phytoplankton blooms did not stand out clearly in the CDOM parameters.

3.3 Chlorophyll-a concentration

The chl-a concentration, as measured with the CTD fluorometer, ranged mostly between 0–7 µg l^{-1} in both the Johor River and the Johor Strait, with the exception of five samples in the Johor Strait that had concentrations of 10.1–50.3 µg l^{-1} (Fig. 4a). These were at stations 5, 6, 7 and 8 in February 2018, and at station 7 in June 2018, indicating that two phytoplankton blooms
235   took place in the inner part of the Johor Strait. Leaving aside these five stations, the chl-a concentration showed no seasonal pattern in the Johor River or the Johor Strait.

The chl-a concentration was not significantly correlated with DOC concentration in the Johor River. In the Johor Strait, the concentration of DOC showed a clear linear relationship to chl-a concentration for the five bloom stations where chl-a exceeded
240   10 µg l^{-1} (y = 1.95x + 105.4, r^2 = 0.92, p = 0.01). Excluding the five bloom stations, there was still a significant correlation between DOC and chl-a concentrations in the Johor Strait (rho = 0.41, p = 0.001; Fig. 4b). This pattern was not seen with a_{350} or with S$_{275-295}$ (no significant correlations), and the five bloom stations had a_{350} values that were close to the overall mean a_{350} for the Johor Strait (1.19 ± 0.39 m^{-1}), but with consistently low S$_{275-295}$ (Fig. 4c,d). However, the bloom stations showed a decreasing trend of SUVA$_{254}$ with chl-a concentration (although this was not statistically significant), and had relatively low
245   SUVA$_{254}$ compared to the other Johor Strait data (Fig. 4e).
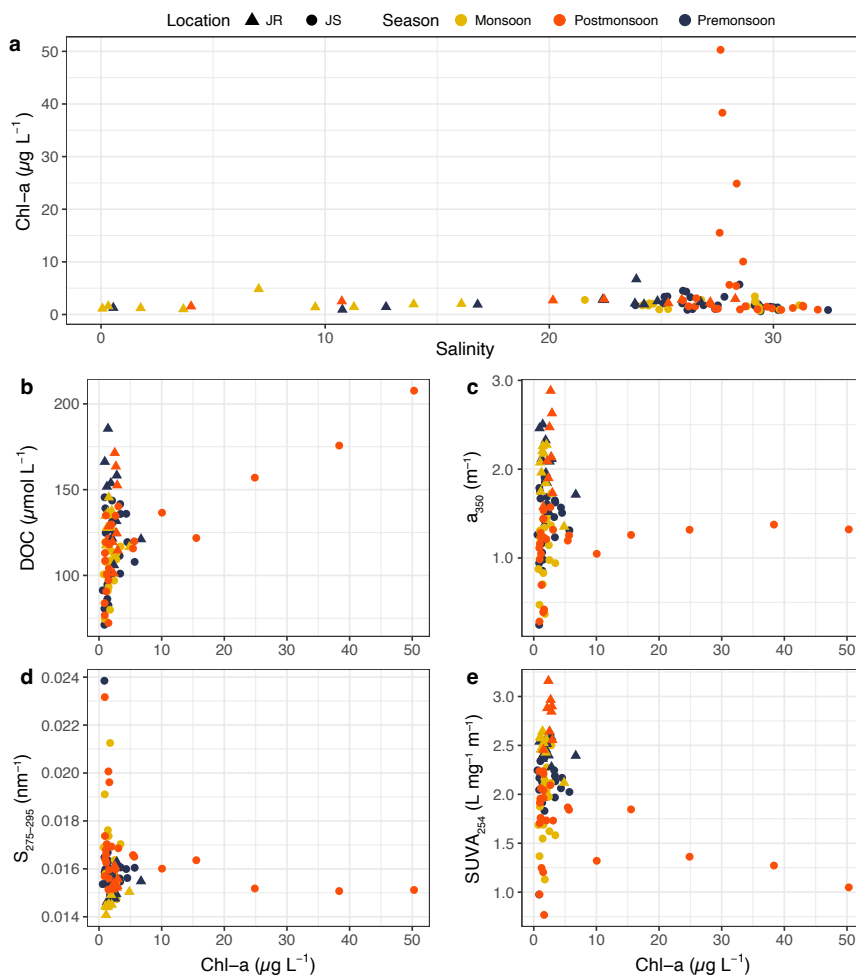
Figure 4. (a) Distribution of chlorophyll-a concentration against salinity. Scatter plots against chlorophyll-a concentration of (b) DOC concentration, (c) CDOM a_{350}, (d) CDOM spectral slope $S_{275-295}$, (e) SUVA$_{254}$. Triangles represent data from the Johor River, circles represent data from the Johor Strait, and symbol colours indicate sampling season.

250

3.4. Relationships between dissolved organic matter parameters

There was a significant correlation between a_{350} and DOC concentration across all sampling seasons and stations (Spearman's rank correlation, rho = 0.69, p < 0.001, Fig. 5a), although the Johor River stations typically had higher a_{350} at a given DOC concentration than the Johor Strait stations. The CDOM spectral slope $S_{275-295}$ and the slope ratio S_R both showed negative

255   correlations with DOC concentration (rho = -0.40, p < 0.001, and rho = -0.49, p < 0.001, respectively; Figs. 5b,c). A strong inverse correlation was observed between $S_{275-295}$ and SUVA$_{254}$ (Spearman's rank correlation, rho = -0.71, p < 0.001, Fig. 5d). The five Johor Strait bloom stations mostly had lower a_{350} and SUVA$_{254}$ relative to the amount of DOC as compared to the other data, but did not have notably different $S_{275-295}$ or S_R (compare Figs. 5a,d to Figs. 5b,c).
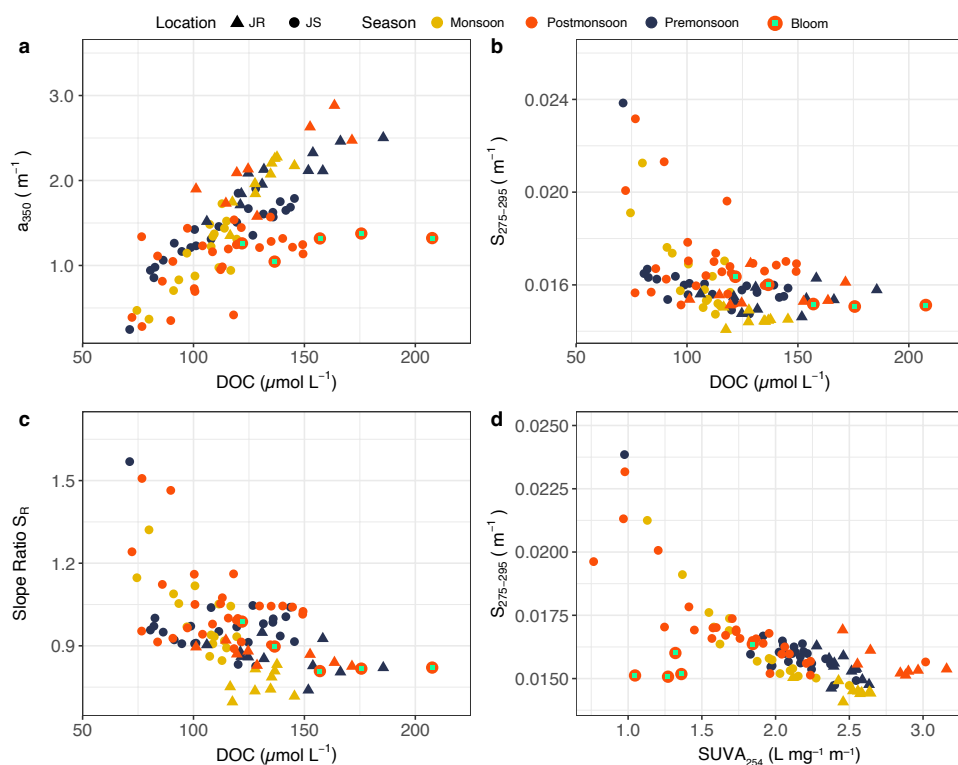
260

Figure 5. Scatter plots to show correlations between (a) CDOM a$_{350}$ and DOC concentration, (b) CDOM spectral slope S$_{275-295}$ and DOC concentration, (c) CDOM spectral slope ratio and DOC concentration, and (d) CDOM spectral slope S$_{275-295}$ and SUVA$_{254}$. Triangles represent data from the Johor River, circles represent data from the Johor Strait, and symbol colour indicates sampling
265 **season. Data from the five bloom stations are indicated by larger symbol size and a light-green rectangle in the point centre.**

3.5 Dissolved inorganic nutrients

The NO$_3^-$ concentration showed a strong and linear decrease with salinity (y = -1.67x + 51.6, r^2 = 0.91, p < 0.001), ranging from 3.1–59.7 µmol l^{-1} in the Johor River and from 0.3–15.2 µmol l^{-1} in the Johor Strait (Fig. 6a). There was no clear seasonal
270 variation in the relationship of [NO$_3^-$] to salinity, although some pre- and post-monsoon samples in the Johor River estuary had lower [NO$_3^-$] than the monsoon samples.

In contrast, the NO$_2^-$ concentration showed a clear enrichment at salinities between 10–27 in both the Johor River and Johor Strait, reaching concentrations of 5–10 µmol l^{-1} (Fig. 6b). At all stations with salinities >31, [NO$_2^-$] was <0.53 µmol l^{-1}, reaching
275 as low as 0.014 µmol l^{-1}, but was always detectable. The highest [NO$_2^-$] were found in the pre- and post-monsoon samples in the Johor River, suggesting that there might be a seasonal pattern (Fig. 6b). Moreover, there was a significant correlation between [NO$_2^-$] and water temperature, although the correlation was fairly weak (rho = 0.278, n=94, p=0.008) (Fig. 6c).

The concentration of NH$_4^+$ generally decreased with salinity in the Johor River (rho = -0.83, p<0.001), with values ranging
280 from undetectable to 39 µmol l^{-1} (Fig. 6d). In the Johor Strait, [NH$_4^+$] was low at salinities ≥30 (undetected to 2.8 µmol l^{-1}), but very variable at salinities of 20–30 (undetected to 51.5 µmol l^{-1}; Fig. 6d), with an overall negative correlation between [NH$_4^+$] and salinity (rho = -0.56, p<0.001). NH$_4^+$ concentrations did not show a seasonal pattern.

PO_4^{3-} concentrations were very low in the Johor River, always <0.4 µmol l^{-1} and in numerous cases <0.05 µmol l^{-1}, and even showed a weak positive correlation with salinity (rho = 0.47, p = 0.01). In the Johor Strait, [PO_4^{3-}] showed a pattern similar to [NH_4^+], with low concentrations (<0.34 µmol l^{-1}) at salinities ≥30, and variable concentrations (<0.05 to 2.7 µmol l^{-1}) at salinities between 20–30 (Fig. 6e). There was an overall negative correlation between [PO_4^{3-}] and salinity (rho = -0.48, p < 0.001). Unlike the strong [NO_3^-]–salinity relationship (Fig. 6a), [PO_4^{3-}] did not show an overall significant relationship to salinity across the Johor River and Johor Strait. PO_4^{3-} concentration did not show any seasonal variation.
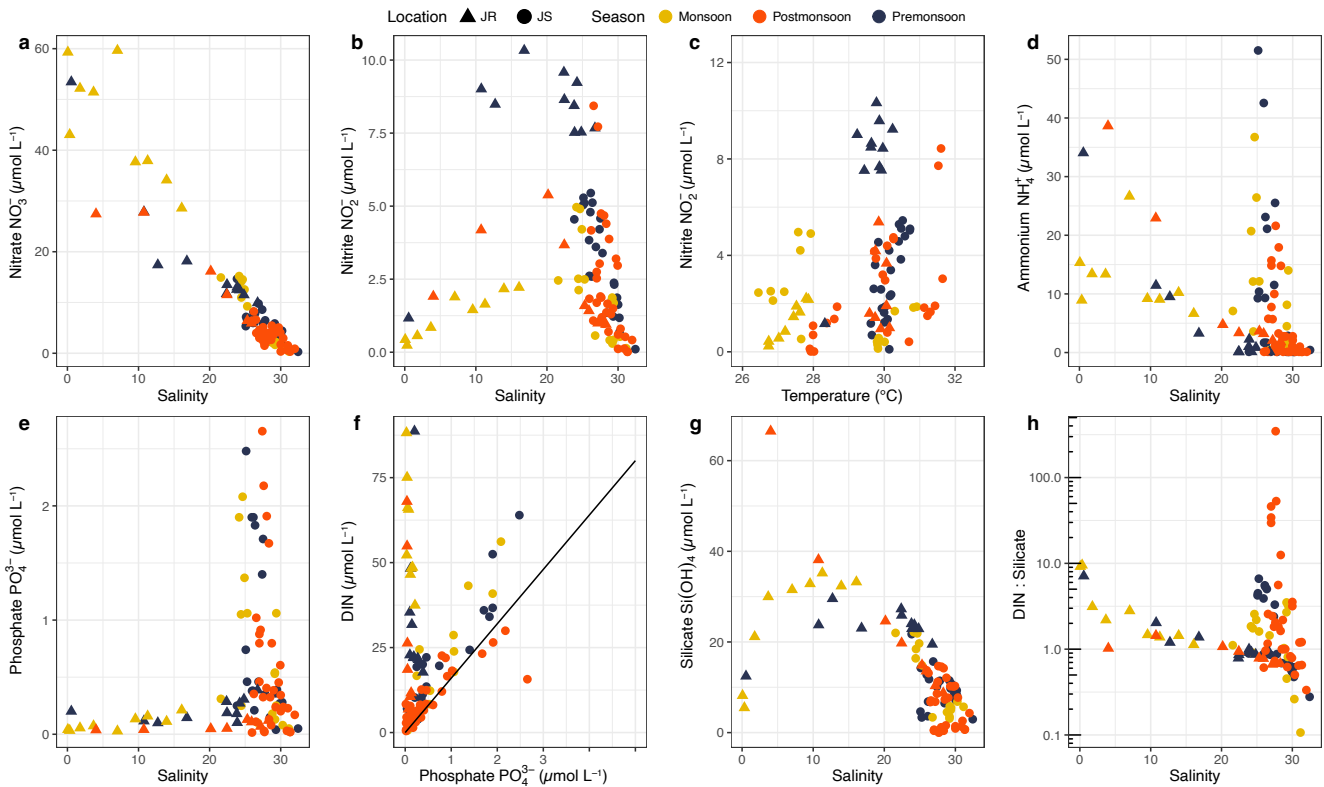
Figure 6. Concentrations of (a) nitrate and (b) nitrite against salinity. (c) Nitrite concentration showed a significant correlation with temperature (Spearman's rank correlation). Concentrations of (d) ammonium and (e) phosphate against salinity. (f) Dissolved inorganic nitrogen was generally correlated with phosphate concentration in the Johor Strait, but not in the Johor River where phosphate concentrations were very low. Solid line indicates 16:1 Redfield ratio. (g) Concentration of silicate against salinity. The very low silicate concentration for low-salinity Johor River samples are likely an artefact of sample freezing; see discussion in Section 4.2. (h) Ratio of dissolved inorganic nitrogen to silicate against salinity. In all panels, triangles represent data from the Johor River, circles represent data from the Johor Strait, and symbol colour indicates sampling season.

In the Johor River, there was consequently no clear DIN–PO_4^{3-} relationship (in fact, a weak negative correlation was seen, rho = -0.43, p = 0.02) and the DIN:PO_4^{3-} ratio was almost always greater than the Redfield ratio of 16:1. In contrast, the Johor Strait data did show a linear relationship between [DIN] and [PO_4^{3-}] (y = 17.3x + 3.4, r^2 = 0.72, p < 0.001), with most data either close to or slightly greater than a 16:1 ratio and a regression slope of 17.3 (Fig. 6f). This suggests an environment in the Johor Strait that is slightly enriched in N as compared to P. The relationship was mainly driven by the relationship between [NH_4^+] and [PO_4^{3-}], which followed the Redfield ratio of 16:1 fairly closely (y = 13.3x – 1.5, r^2 = 0.73, p < 0.001).

The Si(OH)$_4$ concentration was overall negatively correlated with salinity, reaching values <1 µmol l^{-1} at high salinities (rho = -0.69, p < 0.001; Fig. 6g). Although the lowest-salinity samples in the Johor River mostly had low [Si(OH)$_4$] of <10–15 µmol

310 l^{-1} (except for one high measurement of 66.5 µmol l^{-1}), this is most likely an artefact caused by silicon polymerisation in low-salinity samples, as discussed in Section 4.2. The DIN:Si ratios in the Johor River were mostly between 0.7–3.1, with the lowest-salinity stations reaching 7.1–10, while the Johor Strait samples ranged mostly between 0.2–6.0. The highest DIN:Si ratios (12–347) were seen at Johor Strait stations 6–8 in February 2018, which were also the stations with highest chl-a concentration (>25 µmol L^{-1}). Overall, most stations exhibited an excess of DIN relative to the canonical Redfield DIN:Si ratio

315 of 1:1. Within the Johor Strait, stations 6–8 typically had higher concentrations of NO_2^- (1.5–4.8-fold higher), NH_4^+ (3.9–148-fold higher) and PO_4^{3-} (1.2–12-fold higher) than the other stations.

4 Discussion

4.1 Sources and mixing pattern of dissolved organic matter

DOC concentrations observed in the Johor River (115–150 µmol l^{-1}) are at the lower end of values reported from river systems

320 in Malaysia and Indonesia (Huang et al. 2017), where rivers draining tropical peatlands can carry 1000–5000 µmol l^{-1} (Alkhatib et al., 2007; Wit et al., 2015; Martin et al., 2018). The Johor River values are closer to those reported upstream of peatlands in the Rajang River (~120 µmol l^{-1}; Martin et al., 2018) and is consistent with a previously reported wet season value from the Johor River of 214 µmol l^{-1} (Huang et al., 2017). Our comparatively low values of CDOM absorption, with a_{350} <2.5 m^{-1} at the lowest salinities in the Johor River, are also a contrast to the extremely CDOM-rich blackwater rivers found in peatland-

325 draining catchments in Southeast Asia (Martin et al., 2018; Siegel et al., 2019), as well as in Africa (e.g. the Congo River and its tributaries; Spencer et al., 2009; Drake et al. 2023) and South America (e.g. the Orinoco River; Battin, 1998). Neither DOC nor a_{350} followed a conservative mixing pattern, with significant DOM addition happening both within the Johor River estuary and in the Johor Strait.

330 The low values of $S_{275-295}$ (mostly below 0.016 nm^{-1}; Fig. 3d), S_R (all below 1.0; Fig 3f), and elevated $SUVA_{254}$ (all higher than 2 $l mg^{-1} m^{-1}$; Fig. 3c) are consistent with a predominantly terrestrial DOM source within the Johor River estuary. These CDOM parameters are used widely to trace terrigenous DOM in estuaries and river-influenced coastal seas (Fichot and Benner, 2011; Lu et al., 2016; Clark and Mannino, 2021). $SUVA_{254}$ is proportional to the DOM aromaticity (Weishaar et al., 2003) and terrigenous DOM typically has high $SUVA_{254}$ with values above 2 $l mg^{-1} m^{-1}$ (Massicotte et al., 2017). $SUVA_{254}$ was also found

335 to be relatively robust at distinguishing terrigenous from aquatic DOM in decomposition experiments (Lee et al., 2018). $S_{275-295}$ is inversely proportional to the apparent molecular weight of DOM (Helms et al., 2008). S_R also correlates with DOM apparent molecular weight, and has been described as a suitable proxy to distinguish terrestrial and marine CDOM, with marine-like CDOM having S_R >1 (Helms et al., 2008; Helms et al., 2014). However, Han et al. (2021) found that in a temperate estuary system in Korea, S_R was actually elevated (~1.3) in samples richer in terrigenous DOM, which they attributed to prior

340 decomposition. While this indicates that caution is needed when interpreting DOM optical properties as source indicators, we also note that the relatively low concentrations of chl-a in the Johor River (Fig. 4) suggest that autochthonous production is probably not a major source of DOM. Moreover, the high turbidity in the Johor River (total suspended matter concentrations at our stations were typically 10–30 mg l^{-1}; Liang et al., 2020) make it unlikely that submerged vegetation or macroalgae contribute substantially to the DOM pool. However, fringing mangroves are found along much of the Johor River estuary, and

345 mangroves are known to provide large inputs of terrigenous DOM (Jennerjahn and Ittekkot, 2002; Dittmar et al., 2006). An input of terrigenous DOM from these fringing mangroves would help to explain the observed non-conservative mixing pattern in the DOC concentration and CDOM properties (Fig. 3).

The values of the CDOM properties were more variable in the Johor Strait compared to the Johor River. The low values of $S_{275-295}$ and S_R in most of these samples (below 0.018 nm^{-1} and 1.1, respectively), are typically associated with terrigenous DOM in river-influenced coastal margins (Fichot and Benner, 2011; Carr et al., 2019; Lønborg et al., 2021a; Zhou et al., 2021). The low surface salinities in the Johor Strait found in the present study and reported previously (Gin et al., 2000; Kok and Leong, 2019; Mohd-Din et al., 2020) suggest that terrigenous DOM input from runoff probably does contribute to the DOM pool in the strait, while the fringing mangroves along the strait will also supply terrigenous DOM. However, the SUVA$_{254}$ values were mostly lower in the Johor Strait than in the Johor River estuary at a given salinity, which points to an increasing contribution from autochthonous DOM. Given the eutrophic status of the Johor Strait (Gin et al., 2000; Chénard et al., 2019; Kok and Leong, 2019), autochthonous DOM production is likely substantial. This is evident from the high DOC concentrations at the five bloom stations (Figs. 3a, 3b), but also demonstrated by the bottom water hypoxia and sedimentary anoxia found in both the West and East Johor Strait (Kok and Leong, 2019; Chai et al., 2021). However, the phytoplankton bloom did not appear to contribute much CDOM, given that the a_{350} showed little change with chl-a concentration (Fig. 4c). This would explain the low SUVA$_{254}$ relative to $S_{275-295}$ of the bloom stations (Fig. 5d), because production of mostly non-coloured DOM by the bloom would lower SUVA$_{254}$ without influencing $S_{275-295}$. Our data therefore suggest that direct production by phytoplankton is probably not a major source of CDOM in the Johor Strait. This leaves production by heterotrophic microbes as a more likely pathway of generating autochthonous CDOM, given that the hypoxia in the inner part of the Johor Strait (Mohd-Din et al., 2020; Chai et al., 2021) clearly indicates that heterotrophic reprocessing of organic matter is substantial. CDOM produced by microbial reprocessing of DOM can have absorbance and fluorescence properties that resemble terrigenous CDOM (Hansen et al., 2016; Osburn et al., 2019).

4.2 Nutrient sources and implications for phytoplankton dynamics

Although the NO$_3^-$ concentration showed close to linear mixing behaviour across the Johor River and Johor Strait, the pattern of the other nutrients clearly shows that different patterns of nutrient cycling operate in the two locations. Our data indicate that the Johor River is notably enriched in DIN relative to PO$_4^{3-}$. While wastewater treatment plants in the Johor River catchment may be significant point sources of NH$_4^+$ (Pak et al., 2021), the NO$_3^-$ probably originates from soil nitrogen, similar to observations in the Rajang River system on Borneo (Jiang et al., 2019), and possibly from fertiliser use in the largely agricultural catchment. The low PO$_4^{3-}$ concentrations would be consistent with soil nutrient sources, given the predominance of highly weathered acrisol soils in the catchment (Pak et al., 2021) that are likely to be phosphorus-poor. The concentrations of NO$_3^-$ and NH$_4^+$ are broadly in line with values reported from other river systems in tropical and subtropical Asia with varying degrees of anthropogenic impacts, which can reach from 10s to 100s of µmol l^{-1} (Jennerjahn et al., 2004; Cai et al., 2015; Kuo et al., 2017; Suratman et al., 2018; Jiang et al., 2019). The clear increase in NO$_2^-$ concentration at salinities between 10–25 (Fig. 6b) indicates active nitrogen recycling within the Johor River estuary and in the Johor Strait, likely from nitrification of the NH$_4^+$ pool. In a subtropical North American estuary, Schaefer and Hollibaugh (2017) reported that NO$_2^-$ oxidation rates slowed relative to NH$_4^+$ oxidation rates at temperatures of 20–30°C, leading to similar accumulation of NO$_2^-$ as in our data. Whether this temperature-dependent mechanism uncoupling the two steps of nitrification also applies in permanently warm tropical systems is unknown. Our data do show a significant, albeit weak, correlation between NO$_2^-$ concentration and temperature, which suggests that the temperature-sensitivity of biogeochemical rates in tropical estuaries would be an important topic for future research.

The accumulation of NH_4^+ and PO_4^{3-} in the Johor Strait in proportions following the Redfield ratio (Figs. 6d,e,f) suggests that substantial internal recycling of nutrients takes place in the strait; the importance of recycling is also evident from the accumulation of NO_2^- at lower salinities (Fig. 6b). Elevated concentrations of NH_4^+, PO_4^{3-}, and NO_2^- were found especially at Stations 6–8, closer to the inner Johor Strait. Given that the NH_4^+:PO_4^{3-} ratios were generally fairly close to 16:1 (Fig. 6f), recycling via aerobic respiration is likely important. However, Chai et al. (2021) showed that sedimentary anammox, denitrification, and dissimilatory nitrate reduction to ammonia (DNRA) occur throughout the East and West Johor Straits at rates ranging from <0.5–11 μmol kg^{-1} h^{-1}, and that the sediments contain a large fraction of iron-bound phosphorus. Although denitrification + anammox usually exceeded DNRA, the rate of DNRA always exceeded that of anammox and was between 50% and >100% of the denitrification rate at all but one station. Chai et al. (2021) therefore concluded that there is net sedimentary N loss, but that DNRA also recycles an appreciable fraction of NO_3^- to NH_4^+, and that release of iron-bound P from the sediments might also be important. Our data are consistent with N and P recycling helping to maintain a eutrophic state within the Johor Strait. Further research on pelagic and sedimentary nutrient recycling rates in this system is therefore warranted.

Tropical rivers typically carry high $Si(OH)_4$ concentrations, averaging close to 200 μmol l^{-1} in Asia (Jennerjahn et al., 2006). Our low-salinity samples mostly returned values below 30 μmol l^{-1}, yielding a distinct unimodal relationship with salinity. Although it is possible for diatom growth to deplete $Si(OH)_4$ in freshwater reaches of an estuary, and for dissolution of biogenic silica and of aluminosilicate minerals to be enhanced within the saline reaches of an estuary (Eyre and Balls, 1999; Roubeix et al., 2008a; Roubeix et al., 2008b), it is more likely that our result was an analytical artefact caused by silicon polymerisation in frozen samples, which affects low-salinity samples and samples with high $Si(OH)_4$ concentrations more strongly (MacDonald and McLaughlin, 1982). This is expected to be less of a problem in the higher-salinity Johor Strait samples where $Si(OH)_4$ concentrations were also lower, and which showed a much more consistent relationship with salinity (Fig. 6g). Our Johor Strait data indicate a high DIN:Si ratio, typically >1, which is consistent with previous data from the Johor Strait (Chénard et al., 2019; Kok and Leong, 2019). This contrasts with the consistently low DIN:Si ratios, averaging around 0.3, measured in the Singapore Strait and also using frozen samples (Martin et al., 2022). While the Johor Strait does experience diatom blooms (Mohd-Din et al., 2020; Chai et al., 2021), the excess of N and P relative to Si may favour the growth of non-silicifying phytoplankton, including the harmful dinoflagellate blooms that have been observed in the Johor Strait (Kok and Leong, 2019; Chai et al., 2021). Moreover, the fact that DIN:PO_4^{3-} ratios were generally at or above the 16:1 Redfield ratio suggests that phosphorus may play a role in limiting phytoplankton production in the Johor Strait. This is consistent with the data of Kok and Leong (2019) collected in the East Johor Strait between 2015–2017, who found DIN:PO_4^{3-} ratios fairly close to 16:1, and more recent measurements by Wijaya et al. (2023) in 2020, who found DIN:PO_4^{3-} ratios mostly above 16:1.

We do not know the taxonomic composition of the phytoplankton blooms encountered in February 2018 (Stations 6–8) and June 2018 (Station 7). However, on most sampling dates, chl-a concentrations were not particularly elevated, despite high concentrations of nutrients (DIN 10–50 μmol l^{-1}, PO_4^{3-} 0.5–2.5 μmol l^{-1}). This indicates that factors other than nutrient availability, most likely water column stability, light penetration, and ecological interactions such as grazing or viral lysis, are also important controls over bloom formation in the Johor Strait (Chen et al., 2009; Davidson et al., 2014). The fact that one bloom was observed in February 2018, when rainfall was low and the salinity at the bloom stations was relatively high (27.6– 28.7 compared to an overall range of 24.2–29.4 at these three stations across the sampling period) also suggests that direct freshwater run-off was probably not in itself a key trigger for the bloom. Our data are consistent with a recent analysis of

microbial community variation over 2 months in late 2020, which concluded that phytoplankton biomass in the East Johor Strait is likely under a significant degree of top-down control (Wijaya et al., 2023).

4.3 Seasonal biogeochemical variation

430 Although rainfall and therefore river discharge showed clear seasonal variation, this did not result in strong seasonal variation in the biogeochemical parameters we measured, consistent with previous studies in the Johor Strait (Chénard et al., 2019; Mohd-Din et al., 2020). This is despite the fact that the DOM pool in the Johor River is likely largely of terrigenous origin (based on the optical properties), and terrestrial DOC concentrations are typically expected to increase with river discharge (Raymond & Saiers 2010; Kurek et al., 2022; Drake et al. 2023). The somewhat lower DOC concentrations in the Johor River

435 estuary during the northeast monsoon might indicate a dilution effect due to increased rainfall as observed in peatlands (Clark et al., 2007; Rixen et al., 2016). This was not observed for NO_3^-, possibly indicating that NO_3^- originates from shallower horizons of the soil profile than DOC. However, our sampling in the Johor River was limited to three dates, and did not capture periods of peak river discharge (Fig. 2b), hence the true seasonality in riverine concentrations may have been missed. The only parameter where some seasonality was apparent in our data was NO_2^-, which we hypothesise might be linked to temperature

440 as discussed above in Section 4.2. The Johor River estuary and Johor Strait are thus different from estuaries in the seasonal wet–dry tropical climates, where large seasonal variation in precipitation causes much more pronounced seasonal variation in biogeochemistry (Eyre and Balls, 1999; Pratihary et al., 2009; Burford et al., 2012). Our data also suggest that dissolved nutrient concentrations in the eutrophic Johor Strait are not primarily controlled by seasonal precipitation and runoff patterns, and that phytoplankton blooms in the strait are not purely controlled by nutrient availability.

445

While the seasonal variation in rainfall reflected the long-term average seasonality fairly well, we acknowledge that our study only encompassed one year, and thus the interannual variation is at present unknown. Hydroclimate across Southeast Asia is influenced by both the El Niño Southern Oscillation (ENSO) and the Indian Ocean Dipole (IOD) (e.g., Xiao et al., 2022), although a previous analysis of river discharge data concluded that ENSO alone did not significantly influence the variability

450 of Johor River discharge (Xu et al., 2004). We therefore expect that the main conclusions reached in the present study are probably generalizable across years, but more research is needed to resolve longer-scale temporal variability. Any additional anthropogenic impacts and land-use changes are also likely to further alter biogeochemical cycling in this system, and our data thus provide a valuable baseline against which future data can be compared.

455 The limited seasonal variability observed in the present study contrast with the Singapore Strait directly to the south, where the monsoonal reversal of the prevailing ocean currents delivers a seasonal input of terrigenous DOM and nutrients during the southwest monsoon (Zhou et al., 2021; Martin et al., 2022). Our data further show that the Johor River carries much lower concentrations of DOC but much higher concentrations of NO_3^- compared to the inferred concentrations of the river input that affects the Singapore Strait (around 900 µmol l^{-1} for DOC [Zhou et al., 2021; Chen et al. 2023]; and around 24 µmol l^{-1} for

460 NO_3^- [Martin et al., 2022]). This further supports the conclusion that input from the Johor River has little impact on the biogeochemistry of the Singapore Strait (Zhou et al., 2021; Martin et al., 2022), as also shown for suspended sediment concentrations by van Maren et al. (2014). Based on the seasonality and inferred riverine endmember concentrations, the terrigenous input to the Singapore Strait is instead derived from peatland-draining rivers (Zhou et al., 2021; Martin et al., 2022).

5 Conclusion

The Johor River and Johor Strait are clearly biogeochemically distinct and not simply part of the same estuarine mixing continuum. The Johor River appears to carry mostly terrigenous DOM, although with significant non-conservative additions in the estuary. In the eutrophic Johor Strait, phytoplankton blooms produce autochthonous DOM. Although $SUVA_{254}$ showed lower values in the Johor Strait than the Johor River, the CDOM spectral slope parameters in the Johor Strait were consistent with typical terrigenous values, demonstrating that CDOM optical properties may be ambiguous source indicators in eutrophic waters where heterotrophic microbes are likely producing CDOM as well. Our data further reveal possible evidence for temperature-dependent NO_2^- accumulation in estuarine waters despite the limited seasonal temperature range. The large contribution of NH_4^+ to the DIN pool, with $DIN:PO_4^{3-}$ ratios generally at or above 16:1, indicate that internal nutrient recycling is likely important in the Johor Strait, and that phosphorus may at times be the limiting nutrient in this system.

References

Alkhatib, M., Jennerjahn, T. C., and Samiaji, J.: Biogeochemistry of the Dumai River estuary, Sumatra, Indonesia, a tropical black-water river, Limnol. Oceanogr., 52, 2410–2417, https://doi.org/10.4319/lo.2007.52.6.2410, 2007.

Altieri, A. H., Harrison, S. B., Seemann, J., Collin, R., Diaz, R. J., and Knowlton, N.: Tropical dead zones and mass mortalities on coral reefs, Proc. Natl. Acad. Sci. U.S.A., 114, 3660–3665, https://doi.org/10.1073/pnas.1621517114, 2017.

Asmala, E., Kaartokallio, H., Carstensen, J., and Thomas, D. N.: Variation in Riverine Inputs Affect Dissolved Organic Matter Characteristics throughout the Estuarine Gradient, Front. Mar. Sci., 2, https://doi.org/10.3389/fmars.2015.00125, 2016.

Ballagh, F. E. A., Rabouille, C., Andrieux-Loyer, F., Soetaert, K., Elkalay, K., and Khalil, K.: Spatio-temporal dynamics of sedimentary phosphorus along two temperate eutrophic estuaries: A data-modelling approach, Cont. Shelf Res., 193, 104037, https://doi.org/10.1016/j.csr.2019.104037, 2020.

Baum, A., Rixen, T., and Samiaji, J.: Relevance of peat draining rivers in central Sumatra for the riverine input of dissolved organic carbon into the ocean, Estuar. Coast. Shelf Sci., 73, 563–570, https://doi.org/10.1016/j.ecss.2007.02.012, 2007.

Battin, T. J.: Dissolved organic matter and its optical properties in a blackwater tributary of the upper Orinoco River, Venezuela, Org. Geochem, 28, 561-569, 1998.

Bernard, R. J., Mortazavi, B., and Kleinhuizen, A. A.: Dissimilatory nitrate reduction to ammonium (DNRA) seasonally dominates NO_3 − reduction pathways in an anthropogenically impacted sub-tropical coastal lagoon, Biogeochemistry, 125, 47–64, https://doi.org/10.1007/s10533-015-0111-6, 2015.

Beusen, A. H. W., Bouwman, A. F., Van Beek, L. P. H., Mogollón, J. M., and Middelburg, J. J.: Global riverine N and P transport to ocean increased during the 20th century despite increased retention along the aquatic continuum, Biogeosciences, 13, 2441–2451, https://doi.org/10.5194/bg-13-2441-2016, 2016.

Bianchi, T. S. and Morrison, E. S.: Estuarine Chemistry, in: Crump, B.C., Testa, J.M., Dunton, K.H. (Eds.), Estuarine Ecology, Third edition., John Wiley & Sons, Hoboken, NJ, 36–77 pp., 2023.

Burford, M. A., Webster, I. T., Revill, A. T., Kenyon, R. A., Whittle, M., and Curwen, G.: Controls on phytoplankton productivity in a wet–dry tropical estuary, Estuar. Coast. Shelf Sci., 113, 141–151, https://doi.org/10.1016/j.ecss.2012.07.017, 2012.

Cai, P., Shi, X., Hong, Q., Li, Q., Liu, L., Guo, X., and Dai, M.: Using ^{224}Ra/^{228}Th disequilibrium to quantify benthic fluxes of dissolved inorganic carbon and nutrients into the Pearl River Estuary, Geochim. Cosmochim. Acta, 170, 188–203, https://doi.org/10.1016/j.gca.2015.08.015, 2015.

Carr, N., Davis, C. E., Blackbird, S., Daniels, L. R., Preece, C., Woodward, M., and Mahaffey, C.: Seasonal and spatial variability in the optical characteristics of DOM in a temperate shelf sea, Prog. Oceanogr., 177, 101929, https://doi.org/10.1016/j.pocean.2018.02.025, 2019.

Chai, X., Li, X., Hii, K. S., Zhang, Q., Deng, Q., Wan, L., Zheng, L., Lim, P. T., Tan, S. N., Mohd-Din, M., Song, C., Song, L., Zhou, Y., and Cao, X.: Blooms of diatom and dinoflagellate associated with nutrient imbalance driven by cycling of nitrogen and phosphorus in anaerobic sediments in Johor Strait (Malaysia), Mar. Environ. Res., 169, 105398, https://doi.org/10.1016/j.marenvres.2021.105398, 2021.

Chen, B., Liu, H., Landry, M., Chen, M., Sun, J., Shek, L., Chen, X., and Harrison, P.: Estuarine nutrient loading affects phytoplankton growth and microzooplankton grazing at two contrasting sites in Hong Kong coastal waters, Mar. Ecol. Prog. Ser., 379, 77–90, https://doi.org/10.3354/meps07888, 2009.

Chen, Y., Zhou, Y., and Martin, P. The validity of optical properties as tracers of terrigenous dissolved organic carbon during extensive remineralization in coastal waters. Earth and Space Science Open Archive, https://doi.org/10.22541/essoar.167569645.50641934/v1.

Chénard, C., Wijaya, W., Vaulot, D., Lopes Dos Santos, A., Martin, P., Kaur, A., and Lauro, F. M.: Temporal and spatial dynamics of Bacteria, Archaea and protists in equatorial coastal waters, Sci. Rep., 9, 16390, https://doi.org/10.1038/s41598-019-52648-x, 2019.

Clark, J. B. and Mannino, A.: Preferential loss of Yukon River delta colored dissolved organic matter under nutrient replete conditions, Limnol. Oceanogr., 66, 1613–1626, https://doi.org/10.1002/lno.11706, 2021.

Clark, J. M., Lane, S. N., Chapman, P. J., and Adamson, J. K.: Export of dissolved organic carbon from an upland peatland during storm events: Implications for flux estimates, J. Hydrol., 347, 438–447, https://doi.org/10.1016/j.jhydrol.2007.09.030, 2007.

Coble, P. G.: Marine Optical Biogeochemistry: The Chemistry of Ocean Color, Chem. Rev., 107, 402–418, https://doi.org/10.1021/cr050350+, 2007.

Dai, M., Yin, Z., Meng, F., Liu, Q., and Cai, W.-J.: Spatial distribution of riverine DOC inputs to the ocean: an updated global synthesis, Curr. Opin. Environ. Sustain., 4, 170–178, https://doi.org/10.1016/j.cosust.2012.03.003, 2012.

Davidson, K., Gowen, R. J., Harrison, P. J., Fleming, L. E., Hoagland, P., and Moschonas, G.: Anthropogenic nutrients and harmful algae in coastal waters, J. Environ. Manage., 146, 206–216, https://doi.org/10.1016/j.jenvman.2014.07.002, 2014.

Dittmar, T., Hertkorn, N., Kattner, G., and Lara, R. J.: Mangroves, a major source of dissolved organic carbon to the oceans, Global Biogeochem. Cycles, 20, https://doi.org/10.1029/2005GB002570, 2006.

Dong, L. F., Sobey, M. N., Smith, C. J., Rusmana, I., Phillips, W., Stott, A., Osborn, A. M., and Nedwell, D. B.: Dissimilatory reduction of nitrate to ammonium, not denitrification or anammox, dominates benthic nitrate reduction in tropical estuaries, Limnol. Oceanogr., 56, 279–291, https://doi.org/10.4319/lo.2011.56.1.0279, 2011.

Drake, T. W., Barthel, M., Mbongo, C. E., Mpambi, D. M., Baumgartner, S., Botefa, C. I., Bauters, M., Kurek, M. R., Spencer, R. G. M., McKenna, A.M., Haghipour, N., Ekamba, G. L., Wabakanghanzi, J. N., Eglinton, T. I., Oost, K. V., and Six, J.: Hydrology drives export and composition of carbon in a pristine tropical river. Limnol. Oceanogr., 68, 2476-2491, https://doi.org/10.1002/lno.12436, 2023.

Eyre, B. and Balls, P.: A Comparative Study of Nutrient Behavior along the Salinity Gradient of Tropical and Temperate Estuaries, Estuaries, 22, 313, https://doi.org/10.2307/1352987, 1999.

Fichot, C. G. and Benner, R.: A novel method to estimate DOC concentrations from CDOM absorption coefficients in coastal waters, Geophys. Res. Lett., 38, https://doi.org/10.1029/2010GL046152, 2011.

Gin, K. Y.-H., Lin, X., and Zhang, S.: Dynamics and size structure of phytoplankton in the coastal waters of Singapore, J. Plankton Res., 22, 1465–1484, https://doi.org/10.1093/plankt/22.8.1465, 2000.

Green, S. A. and Blough, N. V.: Optical absorption and fluorescence properties of chromophoric dissolved organic matter in natural waters, Limnol. Oceanogr., 39, 1903–1916, https://doi.org/10.4319/lo.1994.39.8.1903, 1994.

Han, H., Hwang, J., and Kim, G.: Characterizing the origins of dissolved organic carbon in coastal seawater using stable carbon isotope and light absorption characteristics, Biogeosciences, 18, 1793–1801, https://doi.org/10.5194/bg-18-1793-2021, 2021.

Hansen, A. M., Kraus, T. E. C., Pellerin, B. A., Fleck, J. A., Downing, B. D., and Bergamaschi, B. A.: Optical properties of dissolved organic matter (DOM): Effects of biological and photolytic degradation. Limnol. Oceanogr., 61, 1015-1032, https://doi.org/10.1002/lno.10270, 2016.

Hansen, M. C., Potapov, P. V., Moore, R., Hancher, M., Turubanova, S. A., Tyukavina, A., Thau, D., Stehman, S. V., Goetz, S. J., Loveland, T. R., Kommareddy, A., Egorov, A., Chini, L., Justice, C. O., and Townshend, J. R. G.: High-Resolution Global Maps of 21st-Century Forest Cover Change, Science, 342, 850–853, https://doi.org/10.1126/science.1244693, 2013.

Helms, J. R., Stubbins, A., Ritchie, J. D., Minor, E. C., Kieber, D. J., and Mopper, K.: Absorption spectral slopes and slope ratios as indicators of molecular weight, source, and photobleaching of chromophoric dissolved organic matter, Limnol. Oceanogr., 53, 955–969, https://doi.org/10.4319/lo.2008.53.3.0955, 2008.

Helms, J. R., Mao, J., Stubbins, A., Schmidt-Rohr, K., Spencer, R. G. M., Hernes, P. J., and Mopper, K.: Loss of optical and molecular indicators of terrigenous dissolved organic matter during long-term photobleaching, Aquat. Sci., 76, 353–373, https://doi.org/10.1007/s00027-014-0340-0, 2014.

Huang, T. H., Chen, C. T. A., Tseng, H. C., Lou, J. Y., Wang, S. L., Yang, L., Kandasamy, S., Gao, X., Wang, J. T., Aldrian, E., Jacinto, G. S., Anshari, G. Z., Sompongchaiyakul, P., and Wang, B. J.: Riverine carbon fluxes to the South China Sea, J. Geophys. Res. Biogeosci., 122, 1239–1259, https://doi.org/10.1002/2016JG003701, 2017.

Huffman, G., Bolvin, D., Braithwaite, D., Hsu, R., Joyce, R., Xie, P.: Integrated Multi-Satellite Retrievals for GPM (IMERG), version 4.4. NASA's Precipitation Processing Center. https://gpm.nasa.gov/data/imerg, 2014

Jennerjahn, T. C.: Biogeochemical response of tropical coastal systems to present and past environmental change, Earth Sci. Rev., 114, 19–41, https://doi.org/10.1016/j.earscirev.2012.04.005, 2012.

Jennerjahn, T. C. and Ittekkot, V.: Relevance of mangroves for the production and deposition of organic matter along tropical continental margins, Naturwissenschaften, 89, 23–30, https://doi.org/10.1007/s00114-001-0283-x, 2002.

Jennerjahn, T. C., Ittekkot, V., Klöpper, S., Adi, S., Purwo Nugroho, S., Sudiana, N., Yusmal, A., Prihartanto, and Gaye-Haake, B.: Biogeochemistry of a tropical river affected by human activities in its catchment: Brantas River estuary and coastal waters of Madura Strait, Java, Indonesia, Estuar. Coast. Shelf Sci., 60, 503–514, https://doi.org/10.1016/j.ecss.2004.02.008, 2004.

575   Jennerjahn, T. C., Knoppers, B. A., Souza, W. F. L., Brunskill, G. J., and Silva, E. I. L. (2006). Factors controlling dissolved silica in tropical rivers. In: Ittekkot, V., Unger, D., Humborg, C., and Tac An, N. (eds.): The Silicon Cycle: Human Perturbations and Impacts on Aquatic Systems, 29-51, Island Press, 2006.

Jiang, S., Müller, M., Jin, J., Wu, Y., Zhu, K., Zhang, G., Mujahid, A., Rixen, T., Muhamad, M. F., Sia, E. S. A., Jang, F. H. A., and Zhang, J.: Dissolved inorganic nitrogen in a tropical estuary in Malaysia: transport and transformation,
580   Biogeosciences, 16, 2821–2836, https://doi.org/10.5194/bg-16-2821-2019, 2019.

Kang, C. S. and Kanniah, K. D.: Land use and land cover change and its impact on river morphology in Johor River Basin, Malaysia. J. Hydrol. Reg. Stud., 41, 101072, https://doi.org/10.1016/j.ejrh.2022.101072, 2022.

Kérouel, R. and Aminot, A.: Fluorometric determination of ammonia in sea and estuarine waters by direct segmented flow analysis, Mar. Chem., 57, 265–275, https://doi.org/10.1016/S0304-4203(97)00040-6, 1997.

585   Kok, J. W. K. and Leong, S. C. Y.: Nutrient conditions and the occurrence of a *Karenia mikimotoi* (Kareniaceae) bloom within East Johor Straits, Singapore, Reg. Stud. Mar. Sci., 27, 100514, https://doi.org/10.1016/j.rsma.2019.100514, 2019.

Kuo, N.-W., Jien, S.-H., Hong, N.-M., Chen, Y.-T., and Lee, T.-Y.: Contribution of urban runoff in Taipei metropolitan area to dissolved inorganic nitrogen export in the Danshui River, Taiwan, Environ. Sci. Pollut. Res., 24, 578–590, https://doi.org/10.1007/s11356-016-7825-4, 2017.

590   Kurek, M. R., Stubbins, A., Drake, T. W., Dittmar, T., Moura, J. M. S., Holmes, R. M., Osterholz, H., Six, J., Wabakanghanzi, J. N., Dinga, B., Mitsuya, M., and Spencer, R. G. M.: Organic molecular signatures of the Congo River and comparison to the Amazon. Glob. Biogeochem. Cycles, 36, e2022GB007301, https://doi.org/10.1029/2022GB007301, 2022.

Le Moal, M., Gascuel-Odoux, C., Ménesguen, A., Souchon, Y., Étrillard, C., Levain, A., Moatar, F., Pannard, A., Souchu, P., Lefebvre, A., and Pinay, G.: Eutrophication: A new wine in an old bottle?, Sci. Total Environ., 651, 1–11,
595   https://doi.org/10.1016/j.scitotenv.2018.09.139, 2019.

Lee, M.-H., Osburn, C. L., Shin, K.-H., and Hur, J.: New insight into the applicability of spectroscopic indices for dissolved organic matter (DOM) source discrimination in aquatic systems affected by biogeochemical processes, Water Res., 147, 164–176, https://doi.org/10.1016/j.watres.2018.09.048, 2018.

Li, X., Sardans, J., Hou, L., Gao, D., Liu, M., and Peñuelas, J.: Dissimilatory Nitrate/Nitrite Reduction Processes in River
600   Sediments Across Climatic Gradient: Influences of Biogeochemical Controls and Climatic Temperature Regime, J. Geophys. Res. Biogeosci., 124, 2305–2320, https://doi.org/10.1029/2019JG005045, 2019.

Liang, Y. Q., Annammala, K. V., Martín, P., Yong, E. L., Mazilamani, L. S., and Najib, M. Z. M.: Assessment of Physical-Chemical Water Quality Characteristics and Heavy Metals Content of Lower Johor River, Malaysia, J. Environ. Treat. Tech., 8, 961–966, 2020.

605   Lønborg, C., McKinna, L. I. W., Slivkoff, M. M., and Carreira, C.: Coloured dissolved organic matter dynamics in the Great Barrier Reef, Cont. Shelf Res., 219, 104395, https://doi.org/10.1016/j.csr.2021.104395, 2021a.

Lønborg, C., Müller, M., Butler, E. C. V., Jiang, S., Ooi, S. K., Trinh, D. H., Wong, P. Y., Ali, S. M., Cui, C., Siong, W. B., Yando, E. S., Friess, D. A., Rosentreter, J. A., Eyre, B. D., and Martin, P.: Nutrient cycling in tropical and temperate coastal waters: Is latitude making a difference?, Estuar. Coast. Shelf Sci., 262, 107571, https://doi.org/10.1016/j.ecss.2021.107571,
610   2021b.

Lu, C.-J., Benner, R., Fichot, C. G., Fukuda, H., Yamashita, Y., and Ogawa, H.: Sources and Transformations of Dissolved Lignin Phenols and Chromophoric Dissolved Organic Matter in Otsuchi Bay, Japan, Front. Mar. Sci., 3, https://doi.org/10.3389/fmars.2016.00085, 2016.

MacDonald, R. W. and McLaughlin, F. A.: The effect of storage by freezing on dissolved inorganic phosphate, nitrate and
615   reactive silicate for samples from coastal and estuarine waters, Water Res., 16, 95–104, https://doi.org/10.1016/0043-1354(82)90058-6, 1982.

Martin, P. and Bianchi, T. S.: Organic Carbon Cycling and Transformation. Reference Module in Earth Systems and Environmental Sciences, https://doi.org/10.1016/B978-0-323-90798-9.00061-5, 2023

Martin, P., Cherukuru, N., Tan, A. S. Y., Sanwlani, N., Mujahid, A., and Müller, M.: Distribution and cycling of terrigenous
620   dissolved organic carbon in peatland-draining rivers and coastal waters of Sarawak, Borneo, Biogeosciences, 15, 6847–6865, https://doi.org/10.5194/bg-15-6847-2018, 2018.

Martin, P., Moynihan, M. A., Chen, S., Woo, O. Y., Zhou, Y., Nichols, R. S., Chang, K. Y. W., Tan, A. S. Y., Chen, Y.-H., Ren, H., and Chen, M.: Monsoon-driven biogeochemical dynamics in an equatorial shelf sea: Time-series observations in the Singapore Strait, Estuar. Coast. Shelf Sci., 270, 107855, https://doi.org/10.1016/j.ecss.2022.107855, 2022.

625   Massicotte, P., Asmala, E., Stedmon, C., and Markager, S.: Global distribution of dissolved organic matter along the aquatic continuum: Across rivers, lakes and oceans, Sci. Total Environ., 609, 180–191, https://doi.org/10.1016/j.scitotenv.2017.07.076, 2017.

Mohd-Din, M., Abdul-Wahab, M. F., Mohamad, S. E., Jamaluddin, H., Shahir, S., Ibrahim, Z., Hii, K. S., Tan, S. N., Leaw, C. P., Gu, H., and Lim, P. T.: Prolonged high biomass diatom blooms induced formation of hypoxic-anoxic zones in the
630   inner part of Johor Strait, Environ. Sci. Pollut. Res., 27, 42948–42959, https://doi.org/10.1007/s11356-020-10184-6, 2020.

Neumann, B., Vafeidis, A. T., Zimmermann, J., and Nicholls, R. J.: Future Coastal Population Growth and Exposure to Sea-Level Rise and Coastal Flooding - A Global Assessment, PLoS ONE, 10, e0118571, https://doi.org/10.1371/journal.pone.0118571, 2015.

Pak, H. Y., Chuah, C. J., Yong, E. L., and Snyder, S. A.: Effects of land use configuration, seasonality and point source on water quality in a tropical watershed: A case study of the Johor River Basin, Sci. Total Environ., 780, 146661, https://doi.org/10.1016/j.scitotenv.2021.146661, 2021.

Pratihary, A. K., Naqvi, S. W. A., Naik, H., Thorat, B. R., Narvenkar, G., Manjunatha, B. R., and Rao, V. P.: Benthic fluxes in a tropical estuary and their role in the ecosystem. Estuar. Coast. Shelf Sci., 85, 387–398, https://doi.org/10.1016/j.ecss.2009.08.012, 2009.

Osburn, C. L., Kinsey, J. D., Bianchi, T. S., and Shields, M. R.: Formation of planktonic chromophoric dissolved organic matter in the ocean. Mar. Chem., 209, 1-13, https://doi.org/10.1016/j.marchem.2018.11.010, 2019.

Raymond, P. A., and Saiers, J. E.: Event controlled DOC export from forested watersheds, Biogeochemistry, 100, 197-209, https://doi.org/10.1007/s10533-010-9416-7, 2010.

Regnier, P., Resplandy, L., Najjar, R. G., and Ciais, P.: The land-to-ocean loops of the global carbon cycle, Nature, 603, 401–410, https://doi.org/10.1038/s41586-021-04339-9, 2022.

Rixen, T., Baum, A., Wit, F., and Samiaji, J.: Carbon Leaching from Tropical Peat Soils and Consequences for Carbon Balances, Front. Earth Sci., 4, https://doi.org/10.3389/feart.2016.00074, 2016.

Rixen, T., Wit, F., Hutahaean, A. A., Schlüter, A., Baum, A., Klemme, A., Müller, M., Pranowo, W. S., Samiaji, J., and Warneke, T.: 4 - Carbon cycle in tropical peatlands and coastal seas. In T. C. Jennerjahn, T. Rixen, H. E. Irianto, and J. Samiaji (Eds.), Science for the protection of Indonesian coastal ecosystems (SPICE), pp. 83–142, Elsevier, https://doi.org/10.1016/B978-0-12-815050-4.00011-0, 2022.

Roubeix, V., Rousseau, V., and Lancelot, C.: Diatom succession and silicon removal from freshwater in estuarine mixing zones: From experiment to modelling, Estuar. Coast. Shelf Sci., 78, 14–26, https://doi.org/10.1016/j.ecss.2007.11.007, 2008a.

Roubeix, V., Becquevort, S., and Lancelot, C.: Influence of bacteria and salinity on diatom biogenic silica dissolution in estuarine systems, Biogeochemistry, 88, 47–62, https://doi.org/10.1007/s10533-008-9193-8, 2008b.

Samsudin, M. S., Azid, A., Khalit, S. I., Saudi, A. S. M., and Zaudi, M. A.: River water quality assessment using APCS-MLR and statistical process control in Johor River Basin, Malaysia. Int. J. Adv. Appl. Sci., 4, 84-97, https://doi.org/10.21833/ijaas.2017.08.013, 2017.

Sanwlani, N., Evans, C. D., Müller, M., Cherukuru, N., and Martin, P.: Rising dissolved organic carbon concentrations in coastal waters of northwestern Borneo related to tropical peatland conversion, Sci. Adv., 8, eabi5688, https://doi.org/10.1126/sciadv.abi5688, 2022.

Schaefer, S. C. and Hollibaugh, J. T.: Temperature Decouples Ammonium and Nitrite Oxidation in Coastal Waters, Environ. Sci. Technol., 51, 3157–3164, https://doi.org/10.1021/acs.est.6b03483, 2017.

Siegel, H., Gerth, M., Stottmeister, I., Baum, A., and Samiaji, J.: Remote Sensing of Coastal Discharge of SE Sumatra (Indonesia), in: Remote Sensing of the Asian Seas, edited by: Barale, V., and Gade, M., Springer International Publishing, Cham, 359-376, 2019.

Sinha, E., Michalak, A. M., Calvin, K. V., and Lawrence, P. J.: Societal decisions about climate mitigation will have dramatic impacts on eutrophication in the 21st century, Nat. Commun, 10, 939, https://doi.org/10.1038/s41467-019-08884-w, 2019.

Spencer, R. G. M., Stubbins, A., Hernes, P. J., Baker, A., Mopper, K., Aufdenkampe, A. K., Dyda, R. Y., Mwamba, V. L., Mangangu, A. M., Wabakanghanzi, J. N., and Six, J.: Photochemical degradation of dissolved organic matter and dissolved lignin phenols from the Congo River, J. Geophys. Res., 114, G03010, https://doi.org/10.1029/2009JG000968, 2009.

Stedmon, C. A. and Markager, S.: Behaviour of the optical properties of coloured dissolved organic matter under conservative mixing, Estuar. Coast. Shelf Sci., 57, 973–979, https://doi.org/10.1016/S0272-7714(03)00003-9, 2003.

Stedmon, C. A., and Nelson, N. B.: The Optical Properties of DOM in the Ocean, in: Biogeochemistry of Marine Dissolved Organic Matter (Second Edition), edited by: Carlson, C. A., Academic Press, Boston, 481-508, 2015.

Stibig, H.-J., Achard, F., Carboni, S., Raši, R., and Miettinen, J.: Change in tropical forest cover of Southeast Asia from 1990 to 2010, Biogeosciences, 11, 247–258, https://doi.org/10.5194/bg-11-247-2014, 2014.

Sulu-Gambari, F., Hagens, M., Behrends, T., Seitaj, D., Meysman, F. J. R., Middelburg, J., and Slomp, C. P.: Phosphorus Cycling and Burial in Sediments of a Seasonally Hypoxic Marine Basin, Estuaries and Coasts, 41, 921–939, https://doi.org/10.1007/s12237-017-0324-0, 2018.

Suratman, S., Abdul Aziz, A., Mohd Tahir, N., and Lee, L. H.: Distribution and Behaviour of Nitrogen Compounds in the Surface Water of the Sungai Terengganu Estuary, Southern Waters of South China Sea, Malaysia, Sains Malays., 47, 651–659, https://doi.org/10.17576/jsm-2018-4704-02, 2018.

Teixeira, C., Magalhães, C., Joye, S. B., and Bordalo, A. A.: Response of anaerobic ammonium oxidation to inorganic nitrogen fluctuations in temperate estuarine sediments, J. Geophys. Res. Biogeosci., 121, 1829–1839, https://doi.org/10.1002/2015JG003287, 2016.

Traina, S. J., Novak, J., and Smeck, N. E.: An Ultraviolet Absorbance Method of Estimating the Percent Aromatic Carbon Content of Humic Acids, J. Environ. Qual., 19, 151–153, https://doi.org/10.2134/jeq1990.00472425001900010023x, 1990.

van Maren, D. S., Liew, S. C., and Hasan, G. M. J.: The role of terrestrial sediment on turbidity near Singapore's coral reefs, Cont. Shelf Res., 76, 75–88, https://doi.org/10.1016/j.csr.2013.12.001, 2014.

Vieillard, A. M., Newell, S. E., and Thrush, S. F.: Recovering From Bias: A Call for Further Study of Underrepresented Tropical and Low-Nutrient Estuaries, J. Geophys. Res. Biogeosci., 125, e2020JG005766, https://doi.org/10.1029/2020JG005766, 2020.

695 Voss, M., Wannicke, N., Deutsch, B., Bronk, D., Sipler, R., Purvaja, R., Ramesh, R., and Rixen, T.: Internal Cycling of Nitrogen and Nitrogen Transformations, in: Treatise on Estuarine and Coastal Science, Elsevier, 231–259, https://doi.org/10.1016/B978-0-12-374711-2.00508-8, 2011.

Weishaar, J. L., Aiken, G. R., Bergamaschi, B. A., Fram, M. S., Fujii, R., and Mopper, K.: Evaluation of Specific Ultraviolet Absorbance as an Indicator of the Chemical Composition and Reactivity of Dissolved Organic Carbon, Environ. Sci.
700 Technol., 37, 4702–4708, https://doi.org/10.1021/es030360x, 2003.

Wijaya, W., Suhaimi, Z., Chua, C. X., Sunil, R. S., Kolundžija, S., Rohaizat, A. M. B., Azmi, N. B. Md., Hazrin-Chong, N. H., and Lauro, F. M.: Frequent pulse disturbances shape resistance and resilience in tropical marine microbial communities, ISME Commun., 3, 55, https://doi.org/10.1038/s43705-023-00260-6, 2023.

Wit, F., Müller, D., Baum, A., Warneke, T., Pranowo, W. S., Müller, M., and Rixen, T.: The impact of disturbed peatlands on
705 river outgassing in Southeast Asia, Nat. Commun., 6, 10155, https://doi.org/10.1038/ncomms10155, 2015.

Xiao, H.-M., Lo, M.-H., and Yu, J.-Y.: The increased frequency of combined El Niño and positive IOD events since 1965s and its impacts on maritime continent hydroclimates. Sci. Rep., 12, 7532, https://doi.org/10.1038/s41598-022-11663-1, 2022.

Xu, Z. X., Takeuchi, K., and Ishidaira, H.: Correlation between El Niño–Southern Oscillation (ENSO) and precipitation in South-east Asia and the Pacific region. Hydrol. Process., 18, 107-123, https://doi.org/10.1002/hyp.1315, 2004.

710 Zhou, Y., Evans, C. D., Chen, Y., Chang, K. Y. W., and Martin, P.: Extensive Remineralization of Peatland-Derived Dissolved Organic Carbon and Ocean Acidification in the Sunda Shelf Sea, Southeast Asia, J. Geophys. Res. Oceans, 126, e2021JC017292, https://doi.org/10.1029/2021JC017292, 2021.

Zhu, G., Wang, S., Wang, W., Wang, Y., Zhou, L., Jiang, B., Op Den Camp, H. J. M., Risgaard-Petersen, N., Schwark, L., Peng, Y., Hefting, M. M., Jetten, M. S. M., and Yin, C.: Hotspots of anaerobic ammonium oxidation at land–freshwater
715 interfaces, Nat. Geosci., 6, 103–107, https://doi.org/10.1038/ngeo1683, 2013.

Acknowledgements

We are grateful to Chen Shuang and Ashleen Tan Su Ying for help with sample analysis and field work, and to Anne Leong and Tan Keng Meng for logistical support during field work. We thank the two anonymous reviewers for constructive feedback
720 that improved the original manuscript. This work was funded through the Singapore Ministry of Education Academic Research Fund Tier 2 (grant MOE-MOET2EP10121-0007) and through a Nanyang Technological University Start-Up Grant.

Data availability

All raw data and analysis codes are available via the NTU Data Repository under https://doi.org/10.21979/N9/XJWPHI

Competing Interests

725 The contact author has declared that none of the authors has any competing interests